Research Article

Triacetin as Lubricant Additive: Slipping Friction between Metal Pairs under Boundary Lubrication

Wattanapat Kumwannaboon and Sathaporn Chuepeng*
ATAE Research Unit, Department of Mechanical Engineering, Faculty of Engineering at Sriracha, Kasetsart University, Chon Buri, Thailand

Cholada Komintarachat
Department of Basic Science and Physical Education, Faculty of Science at Sriracha, Kasetsart University, Chon Buri, Thailand

* Corresponding author. E-mail: schuepeng@eng.src.ku.ac.th DOI: 10.14416/j.asep.2022.01.002
Received: 22 August 2021; Revised: 30 September 2021; Accepted: 12 October 2021; Published online: 7 January 2022

Abstract
Friction between rubbing pairs plays a key role in operating machines in an efficient approach. In some intended works or occasional circumstances, slipping friction may occur during dry or boundary lubrication. Lubricating mechanical equipment using proper and efficient lubricant agents is tremendously necessary. This work explores the synthesized triacetin as an additive for lubricant under slipping friction between steel rollers and aluminum, brass, copper, and stainless-steel rods under boundary lubrication. The metal surface morphology under the lubricant with 10% triacetin additive covering roughness periphery is investigated by Field Emission Scanning Electron Microscope imaging. In the dry slipping condition, the friction coefficient is lower for the copper-steel pair compared to the aluminum-steel combination. Compared to the absence of triacetin additive, the steel roller combinations with the rod metal specimens undergoing boundary lubrication with 10% triacetin additive in the lubricant can reduce the slipping friction coefficient by up to 49.2% in the case of steel roller and brass rod pair. The quantitative influences of triacetin additive on metal rubbing pair friction coefficients under boundary lubrication are inversely exponential correlated to triacetin additive, varying in the range of 0 to 10% v/v.

Keywords: Additives, Boundary, Friction, Lubricant, Metal, Triacetin

1 Introduction

Friction between rubbing pairs plays a key role in operating machines in an efficient approach. Especially, those metal pairs of surfaces under staved or boundary lubrication require proper schemes to mitigate movement resistance [1]. Some examples associated with slipping friction or stick-slip condition comprise meshing gears in automotive gearbox or differential, piston ring and liner, piston skirt and cylinder wall, mechanism bearing, and so on [2]. These applications necessitate certain means of friction reduction, in particular a suitable lubrication oil for rubbing pairs and other environmental and operating conditions. In addition, improving lubricant to be more efficient can help reduce energy loss in fuel-saving [3].

Analysis of friction and lubrication that occurs in between material pair of rubbing, and size, shape, and surface of the material is an important part of studying relative moving behavior and wear [4]. Several research works have been established and published regarding friction in both micro and macro scales as well as slipping and stick-slip frictions. Depending on the shape and type of lubricated contacts, slipping friction is one of the most frequent cases [5]. Flicek *et al.* [6] set up a frictional experiment for a block in elastic square shape sliding on a semi-planar after first normal compression and later applying shear load. At high

shear forces applied that closed to sliding condition, insignificant change of friction coefficient in response was observed. Beyond elasticity, Antoni [7] analogically analyzed in detail between plasticity and friction. Extended from the Coulomb's friction, an equivalent mathematical theory was asymptotically analyzed that can localize on a surface for plastic strain. Under frictional slipping contact conditions, Lu *et al.* [8] analytically disclosed the contact stress in a lined circular tunnel. The tangential stress was founded to scatter over the lining boundary for both inner and outer at diverse coefficients of friction and lateral loads.

In some intended works or occasional circumstances, slipping friction may occur during dry or boundary lubrication [9]. Wang *et al.* [10] conducted theoretical and experimental works that found a friction-induced vibration during the stick-slip situation. A complex dual-pin-on-disc configuration was set up for the experiment, while a new simplified two-degree-of-freedom model for the configuration was also accomplished. Stick-slip oscillation was tested covering normal load range at various disc velocities, and its behavior during vibration was disclosed. In dry sliding friction, oscillation can also happen [11]. However, the friction reduction can be mitigated by imposing synchronized normal load oscillation. From these points of view, increasing lubrication efficiency is overwhelmingly important, especially the high-load and long-time operation of the machine. Lubricating mechanical equipment using proper and efficient lubricant agents is tremendously necessary.

Lubrication oil is principally composed of base oil and additives that help preventing wear and friction between two surfaces in contact with relative movement [12]. Usually, vegetable oils and animal fats are insufficiently stable as a proper base oil in heavy-duty working conditions, while mineral and synthetic oils are more popularly used [13]. However, many additives are obligated to improve some specific properties required for certain work, such as friction modifier [14]. In extreme temperature and pressure applications such as the gas drilling industry, Lan *et al.* [15] found a foreseeable scheme by filling lubricant additives to lower the friction. By comparing between presence and absence of lubricant additives at 3.45 MPa pressure and up to 200 °C temperature, the two tested additives exhibited different load capacity resistances. The viscosity of the drilling fluid has been founded to play a key parameter in defining wear and friction behaviors.

In general, zinc dialkyldithiophosphates (ZDDP) are applied as anti-wear additives as well as a corrosion inhibitor and antioxidant, especially for metal-to-metal contacts. Massoud *et al.* [16] strengthened the lubrication efficiency of the exposed surfaces to prevent wear or reduce friction using ZDDP as an antioxidant agent. Apart from the main functions of lubricant, Zohdi [17] applied micro-scale additives to reduce heat generation in thin film lubrication of bearing. The escalation in temperature of the fluid film between the bearing and housing was related to rotational speed, base oil viscosity, and additives' physical properties, i.e., heat capacity, density, viscosity, and mixing ratio [17], [18]. Recently, nanomaterials have been gained more attention for being additives to liquid lubricants. Wen *et al.* [19] applied graphene-like covalent-organic compounds in two layers as the lubricant additives. The novel findings of the lubricated system created metal ions that promoted a stable adsorbed film formation of the lubricant. During sliding, their very thin layers lowered shear stress that finally reduced wear and friction, respectively, by 95.4% and 53.5% at 0.008% w/w additive dosage. For ceramics surfaces, Cui *et al.* [20] synthesized additives for water-based lubricant from nanoparticle materials. Silicon dioxide nanoparticles homogenously lubricated well with the ceramic surface and meaningfully lowered wear and friction. Meanwhile, zinc oxide and titanium dioxide cannot reach a homogenous protective film formation that resulted in tribological inefficiency. Therefore, to create proper lubricant at higher-level performance, finding other prospect additives to enhance lubricity between metal contact surfaces is crucial.

Triacetin or glycerol triacetate is the tri-ester of glycerol and acetic acid or acetic anhydride [21]. Triacetin is frequently synthesized from glycerol and acetic acid over several acid catalysts [22]. Various types of oils are sources of ester and triacetin production, for example, macaw oil [23], Crambe oil [24], waste cooking oil [25], and so on. Triacetin and its blends can be used in various applications dependent on desired properties [26]. Over a heterogeneous gold catalyst, Delesma *et al.* [27] examined biodiesel production mechanisms using the triacetin transesterification density function. In a common approach, triacetin has been, therefore, usually founded in biodiesel production.

By this convention, Zare *et al.* [28] blended waste cooking oil-based biodiesel with triacetin as a fuel additive to study for exhaust emissions and engine performance. The use of triacetin additive to biodiesel can drastically reduce emission levels.

Most studies have used metal and non-metal as additives for lubrication oil, even for nanomaterial. Meanwhile, limited work has been done on the slipping friction in metal or non-metal rubbing pairs using triacetin additive under boundary lubrication. Additionally, other triacetin properties may be suitable to use as an additive for lubricant. Besides, there is less available information for the quantitative comparison among triacetin additive and type of metal rubbing pairs. In subsequence, some other facets have not yet been discovered regarding these issues.

The first objective of this work is to investigate dry slipping friction on a steel roller with other paired metals in rod-type, i.e., aluminum, brass, copper, and stainless steel. Meanwhile, the second objective is to identify the quantitative influences of triacetin additive on metal surface pair friction under boundary lubrication. The coefficient of friction when mixing the base lubricant with triacetin additive varying in the range of 0 to 10% v/v will be determined and discussed. Based on these findings, an empirical correlation between friction coefficient and triacetin additive amount in lubricant is proposed. By these aims, the lubricant temperature – viscosity dependency will be first determined. In order to insight into physical characteristics, the selected metal surface textures under lubricant with triacetin additive within roughness periphery are also inspected by Field Emission Scanning Electron Microscope (FE-SEM) imaging.

2 Materials and Methods

2.1 *Friction coefficient determination based on slipping friction test*

The relative movement of two objects creates friction. The magnitude of this friction is dependent on the type and characteristics of the material and the test conditions. Therefore, experimental studies to identify the occurrence of this phenomenon will be essential to identify the factors that cause friction. In this work, friction determination is based on the slipping friction test as the apparatus is depicted in Figure 1 with its

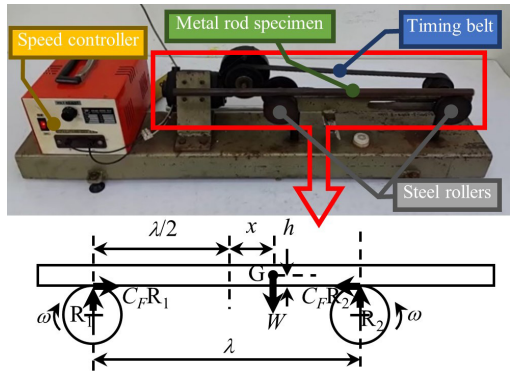

Figure 1: Slipping friction test apparatus and calculation parameters.

concerning parameters.

Figure 1 describes that the two steel rollers are timely rotating in the counter direction. A metal rod of uniform size is placed across the two rollers rotating opposite each other with a constant angular speed ω. The rod's center of gravity (G) moves to the right from the center position between the two rollers, as seen by the x displacement. The reaction forces at the point of contact between the rods and rollers are R_1 and R_2. By applying summation of the moment around G and summation of forces in both vertical and horizontal directions, the equation of motion of the metal rod will be:

$$\frac{d^2x}{dt^2}+\left(\frac{C_F g}{\frac{\lambda}{2}-C_F h}\right)x=0 \tag{1}$$

Where x is horizontal displacement, C_F is slipping friction coefficient, h is the vertical height of the G-point position, and t is time. By solving Equation (1), the solution x is [Equation (2)]:

$$x=C_1\cos\omega t+C_2\cos\omega t \tag{2}$$

with the angular velocity ω of [Equation (3)]:

$$\omega=\sqrt{\frac{C_F g}{\frac{\lambda}{2}-C_F g}} \tag{3}$$

and the period (T) of [Equation (4)]:

$$T = 2\pi\sqrt{\frac{\frac{\lambda}{2} - C_F g}{C_F g}} \quad (4)$$

The slipping friction coefficient C_F is, therefore, calculated by:

$$C_F = \frac{2\pi^2}{gT^2 + 4\pi^2 h} \quad (5)$$

where T is period, g is gravitational acceleration and λ is the specific length between the two roller centers (0.35 m).

2.2 *Base lubricant*

A multi-grade semi-synthetic oil in API SN service classification with SAE 10W-40 viscosity grade was used as the base lubricant. The base lubricant is primarily designed for gasoline cars using gasoline, -blended gasoline fuels, and gas-fueled (compressed natural gas or liquefied petroleum gas) engines. Its main component comprises hydrotreated heavy paraffinic petroleum distillates, whereas treating hydrocarbon compounds on a portion of the petroleum with hydrogen was performed in the presence of a catalyst. Its carbon numbers are principally in the range of C20 to C50, the relatively high saturated hydrocarbons. The key engine lubricant specifications determined by a third-party laboratory are concisely listed in Table 1, with a clear amber color depicted in Figure 2(a).

Table 1: Key properties of the base lubricant

Selected Properties	Method	Unit	Value
Density at 15 °C	ASTM D4052	g/cm^3	0.862
Viscosity at 40 °C	ASTM D445	cSt	97.7
Viscosity at 100 °C	ASTM D445	cSt	14.5
Viscosity index	ASTM D2270		153
Flash point	ASTM D92	°C	226
Pour point	ASTM D5950	°C	–36

2.3 *Triacetin synthesis*

Triacetin in this work was synthesized via acetylation of glycerol that was obtained as a by-product from the production of biodiesel. The glycerol by-product was extracted by hexane three times to remove some traces of biodiesel and unreacted alcohol using a separation funnel. The collected 100-g glycerol used in the acetylation reaction was not further purified due to procedure complications at a cost [29], [30]. In a batch reactor, the triacetin was synthesized from glycerol and acetic acid with a sulfuric acid catalyst impregnated by activated carbon. The acetic acid used in the reaction was anhydrous analytical reagent grade (Merck, 100% purity). The acetylation reaction was carried out in a flask with a two-neck round bottom, reflux condenser, and thermometer under atmospheric pressure. Glycerol and acetic acid, by 1 : 6 molar ratio, were mixed under magnetic stirring and heated to 120 °C by immerging in a constant temperature bath [30]. The reaction started when adding a 4.0% w/w catalyst [30], the activated carbon (10–900 μm in particle size) permeated to sulfuric acid (SAC) [31]. Figure 3 shows the acetylation reaction of glycerol and acetic acid to yield triacetin. After a 3-hour reaction time [30], the flask was immersed in a cold-water bath to quench the reaction, and then the SAC were separated using filtration in a vacuum atmosphere. The triacetin was extracted from the filtrate by hexane with the volumetric ratio of hexane to filtrate by 1:1. Later, they were removed by rotary evaporation before gas chromatography analysis. Figure 4 shows the gas chromatogram of triacetin taken place by the peak at 13.361 min. By GC analysis, the acetylation reaction of glycerol and acetic acid resulted in 86.7% glycerol conversion. As

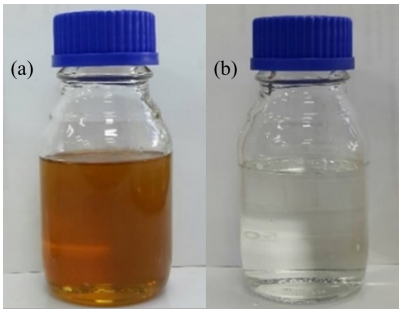

Figure 2: Physical appearance of the substances (a) base lubricant and (b) triacetin, used in the test.

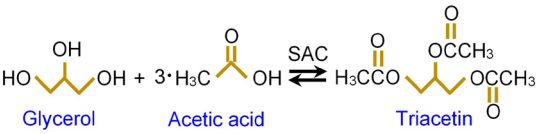

Figure 3: Acetylation of glycerol and acetic acid to triacetin.

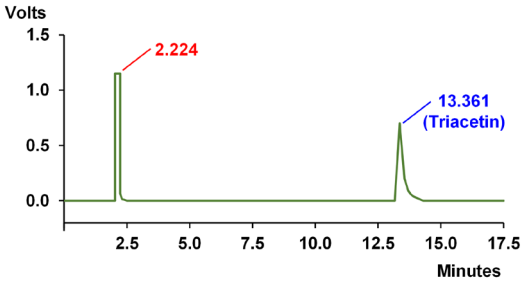

Figure 4: Gas chromatogram of triacetin.

depicted by a clear color in Figure 2(b), the produced triacetin was 98.7% purity with the kinematic viscosity of 9.32 cSt at 40 °C.

2.4 *Metal surface preparation*

Four material types of rod specimens were used for the test, i.e., aluminum, brass, copper, and stainless steel, and their key mechanical properties determined by a third-party laboratory are shown in Table 2. The lengths of each rod type were equivalently set to 0.6 m while their densities were different, resulting in dissimilar mass and hence, mass moment of inertia. It is to note that the mass moment of inertia values indicated in Table 2 are around the axis transverse to the rod. In theory, based on Equation (5), the weight of the rods as the applied load does not affect the slipping friction coefficient. In an experiment, previously attained results of slipping friction coefficients were insignificantly affected by the mass load. In an aspect of geometric dimensioning and tolerancing, surface roughness is a key factor that was already proven to affect friction [32]. All metal surfaces were prepared to reach a peak-to-peak value (R_z) of 1.4 ± 0.1 µm and the average surface value (R_a) of 0.17 ± 0.01 µm. These values of roughness parameters were chosen to conform to EN ISO 4287 standard. In addition, the room temperature was controlled at 30 ± 1 °C as it can affect lubricant distribution and interfacial surfaces [33]. Furthermore, the rotational speed of the steel rollers was kept constant at 200 ± 2 rpm for all material combinations.

To study a physical surface texture under boundary lubrication, a Field Emission Scanning Electron Microscope (FE-SEM) (JEOL, Model JSM-7600F) was employed, at the accelerating voltage and magnification of 20 kV and 10,000 times, respectively.

2.5 *Test conditions and procedure*

Boundary lubrication condition was prepared by applied load (mass of the rods for this work) to the contacting surfaces, mostly asperities of the solids instead of a lubricant [34]. The condition was set by controlling the ratio of the lubricant film thickness to the metal surface roughness by less than unity. This was commissioned by rinsing the lubricant homogeneously mixed with triacetin in the specified ratio onto the rod specimens while slowly spinning around until wetted all over bodies. After that, the soaked rod specimens were removed and left overnight at room temperature to ensure that the lubricant and triacetin mixtures were affixed and met the desired film thickness to the metal surface roughness ratio (<1). To warrant the film thickness, the treated rod specimens were sampled and re-examined by the FE-SEM, where the depth of the lubricant mixture film can be determined, as depicted in Figure 5.

By operating at relatively low slipping velocity, as the bodies of rod and rollers were closely contacted at their asperities, the heat developed by the load may cause a stick-slip condition, and some asperities may break off. During each single test of friction, no additional mixtures of lubricant and triacetin was supplied, only the coated rod specimens were moving on the two steel rollers.

Table 2: Key mechanical properties of the metal materials

Item	Unit	Aluminum	Brass	Copper	Stainless Steel
Yield tensile strength	MPa	103	228	325	215
Ultimate tensile strength	MPa	145	440	385	505
Brinell hardness	kg/mm^2	60	130	107	123
Density	g/l	2,700	8,400	8,890	8,000
Length	m	0.6	0.6	0.6	0.6
Mass	g	317.5	1,007.8	1,064.2	988.6
Mass moment of inertia	kg/m^2	0.9×10^{-2}	3.0×10^{-2}	3.1×10^{-2}	2.9×10^{-2}

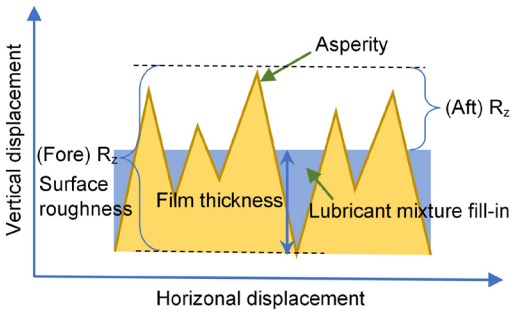

Figure 5: Contacting solid surface.

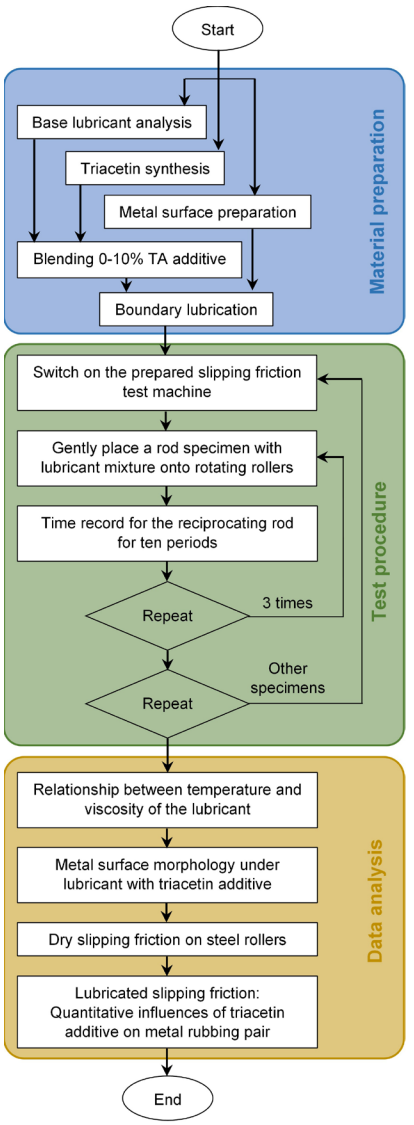

Figure 6: Experimental study flowchart.

Figure 6 shows the experimental study flowchart that includes the steps: material preparation, test procedure, and data analysis. In the material preparation, the provision of base lubricant, triacetin synthesis, and metal surface are previously described in Sections 2.2, 2.3, and 2.4, respectively. The base lubricant was mixed by triacetin additive in a variation of 0, 2, 4, 6, 8, and 10% v/v. These values were selected based on the recommended data in the range of 5–15% additives gathered in [35]. The test procedure was begun by switching on the prepared slipping friction test machine. By gently placing a rod specimen with a fractioned-additive lubricant onto the rotating rollers, time recording for the reciprocating rod for ten periods was accomplished. This step was repeated three times for each rod specimen material. For the measurement of friction coefficient regarding the scheme explained in Section 2.1, every single experimental condition was repeated three times, and averaged values of the friction coefficient are presented here as typical representatives.

For the data analysis illustrated in Figure 6, the relationship between temperature and viscosity of the lubricant was first determined. Later, metal surface morphology under lubricant with triacetin additive was disclosed. Dry slipping friction on steel rollers preceding lubricated slipping friction provided an overview of the initial condition. Lastly, quantitative influences of triacetin additive on metal rubbing pair were explored with relationships between friction coefficient and triacetin additive amount in the lubricant.

3 Results and Discussion

3.1 *Relationship between temperature and viscosity of the lubricant*

The lubricant was first determined for correlation between temperature and viscosity before accomplishing the test. By the standard test method for kinematic viscosity (ASTM D445), in the range of 40 to 100 °C, Figure 7 shows the lubricant kinematic viscosity, which is nonlinear and inversely correlated to the temperature. The thinner lubricant behaves at a high temperature. The temperature-dependent viscosity of the base lubricant can be expressed by the Arrhenius equation as:

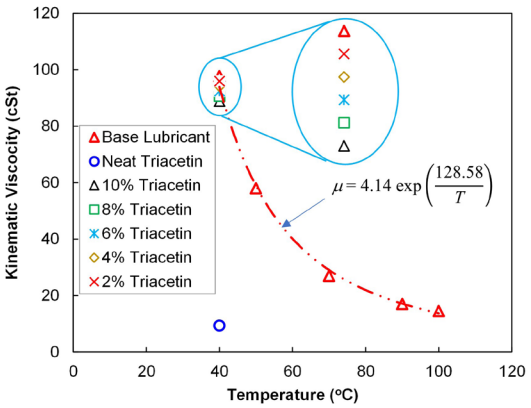

Figure 7: Temperature-viscosity dependency of the base lubricant oil and the lubricant-triacetin mixtures.

$$\mu = 4.14 \exp\left(\frac{128.58}{T}\right) \quad (6)$$

Where T is lubricant temperature in °C and μ is kinematic viscosity in cSt.

Between 40 °C and 100 °C, the attained correlation of viscosity and temperature in Equation (6) was close-fitting by the Arrhenius equation due to the availability of the data set. This is based on Andrade's viscosity of liquids quoted in Messaâdi *et al.* [36].

Figure 7 also shows the kinematic viscosity of the neat triacetin additive derived from the synthesis explained in Section 2.3 for comparison. It is expected that when mixing the base lubricant with a triacetin additive in a variation of up to 10% v/v, the viscosity of the mixture would drop down by some certain extents. The calculated molar average viscosity values of the mixture are also shown in Figure 7.

3.2 *Metal surface morphology under lubricant with triacetin additive*

All the metal surfaces were prepared as essential first stage treatment of substrates before the application of lubricated oil with triacetin additive. The initial surface condition for all materials was largely covered with adhering mill scale with little observed oxidized material. The methods of preparation and grades of cleanliness were associated with hand and power tool cleaning, abrasive blast cleaning, and removal of soluble iron corrosion products. Later, the surface profile and amplitude were treated and controlled to the values mentioned in Section 2.4 ($R_z = 1.4 \pm 0.1$ µm and $R_a = 0.17 \pm 0.01$µm) prior to coating with 10% triacetin additive in lubricant to form boundary lubrication condition.

Figure 8 shows the FE-SEM micrographs of the material surfaces used in the experiment that was coated with 10% triacetin additive mixed with the base lubricant. The scope condition was adjusted to the accelerating voltage and magnification of 20 kV and 10,000 times, respectively. On the surface textures for all materials, the scratches on materials exhibit small shallow grooves where the lubricant with the additive can fill in. These findings resemble to the surfaces reported in [4] but a bit different morphology due to the tribological behavior of lubricants with additive containing copper nanoparticles. It can also be generally seen in Figure 8 that the surface texture grooves of relatively soft materials such as aluminum and copper, compared to the other harder materials: stainless steel and brass, were shallower after being covered by the lubricant with the additive. Usually, for boundary lubrication, layers of lubricant cover valleys and peaks of asperities where the ratio of the lubricant film thickness to the metal surface roughness was less than unity. This condition can help prevent wear and friction, which will be explored in the next sections.

3.3 *Dry slipping friction on steel rollers*

The coefficient of slipping (kinetic) friction in this work is defined as the friction force in the parallel direction to the rubbing surface over normal force acting perpendicular to the rubbing surface. The coefficient of slipping friction is usually higher than the coefficient of static friction [37]. The experiment for dry friction before using triacetin additive among materials used in the tests: aluminum, brass, copper, and stainless steel, on steel rollers was accomplished. This was done on the assumption that the roller speed and the rod specimen mass do not affect the friction coefficient by the theory expressed in Section 2.1. However, the roller rotational speed was kept constant throughout the whole test.

Figure 9 shows the coefficient of friction between unlubricated metal rubbing pairs: aluminum-steel, brass-steel, copper-steel, and stainless steel-steel. The dry friction tested found that most dry materials in combination have the friction coefficient values

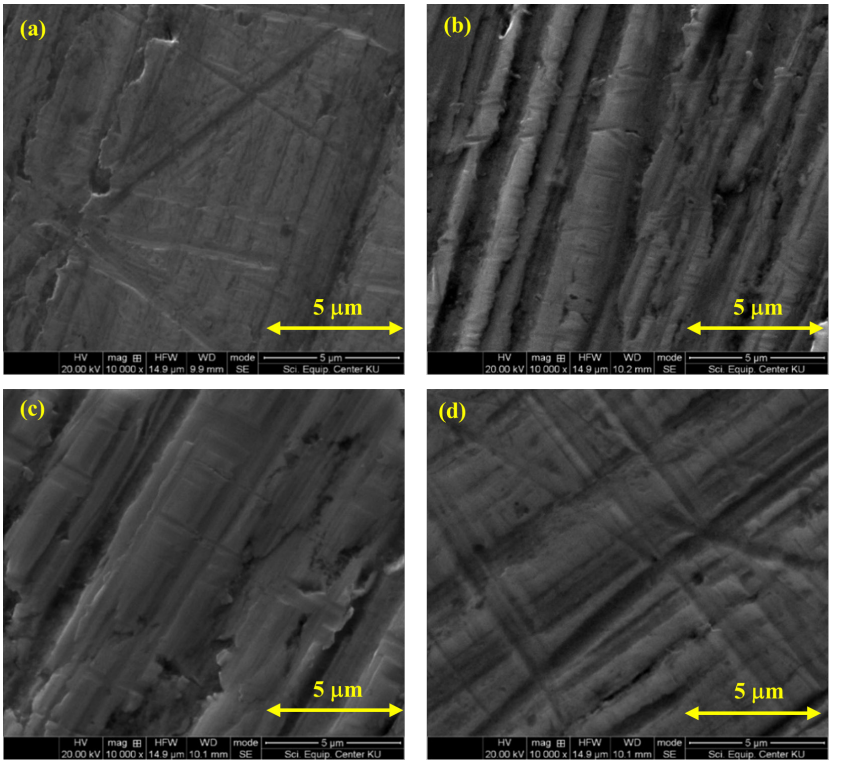

Figure 8: FE-SEM imaging of metal surfaces under boundary lubrication of lubricant with 10% v/v TA additive: (a) aluminum, (b) brass, (c), stainless steel, and (d) copper, 20 kV accelerating voltage and 10,000-time magnification.

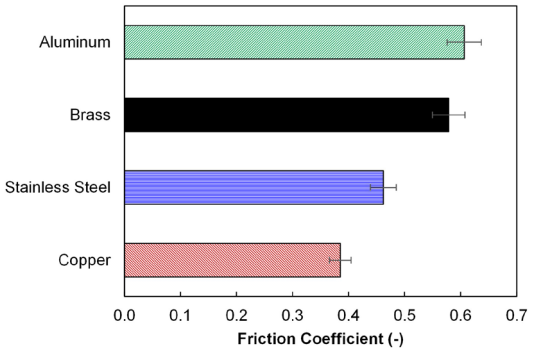

Figure 9: Friction coefficient for dry rubbing pairs of metals versus steel, error bars denoted 5% error amount.

between 0.38 and 0.60. Under the test conditions previously mentioned in Section 2.5, it is founded that the friction coefficient over steel rollers with the rod types: aluminum, brass, stainless steel, and copper are in order from the maximum down to the minimum values of 0.60, 0.57, 0.46 and 0.38, respectively. These different friction coefficient values are related to different mechanical properties as well as test conditions and methods.

To explain the obtained values of dry slipping friction coefficient, the load, sliding speed, temperature, surface finish, wettability, and surface tension must be considered [38]. In this work, the sliding speed, temperature, and surface finish were similarly kept as mentioned in Section 2 as well as the test method used (slipping friction) is theoretically independent of these parameters. However, wettability and surface tension is different depending on the type of materials in combination. In general, materials with high surface tension exhibit high wettability at a high fraction of grain boundary [39]. A high fraction of grain boundary in the sample yielded a low friction coefficient [40]. In comparison, copper and aluminum in liquid form have surface tensions of 1,285 mN/m and 914 mN/m, respectively [41]. In addition, Keene [42] reported in their work on the relationship between electron density and surface tension that copper and aluminum

have surface tensions by approx. 1,300 mN/m and 900 mN/m, respectively. This yields a friction coefficient of copper to be lower than that of aluminum. This theme of explanation is inline with the results attained where the friction coefficient of the steel rollers and brass rod combination lies in between.

3.4 *Lubricated slipping friction: Quantitative influences of triacetin additive on metal rubbing pair*

Figure 10 shows the slipping friction coefficient as a result of triacetin additive variation in lubricant between rubbing pairs of various metals, i.e., aluminum, brass, copper, and stainless steel versus steel under boundary lubrication. The friction coefficient in the graphs with a 5% error amount was reduced with the increasing triacetin from 0 to 10% v/v in the base lubricant for all rubbing pairs tested. For all sets with triacetin proportions after blending for one hour, the base lubricant with additive was homogeneous and did not show any separation. This is due to the fact that both lubricant and triacetin are non-polar, and they are favorable for amalgamation when mixing. When pure lubricant was applied to the rod specimens (0% triacetin additive), the friction coefficient values were in the range of 0.382 to 0.527. The friction coefficient started to decline for all metals after adding triacetin only for 2% v/v and continued to drop throughout 10% addition. At the maximum 10% triacetin additive, the friction coefficient values dropped down to the new range of 0.231 to 0.304. In comparison to the 0% triacetin addition, the pairs of steel – aluminum, – brass, – copper, and – stainless steel undergoing boundary lubrication at 10% triacetin additive in the lubricant are shown to reduce the friction coefficient by 44.6, 49.2, 20.4 and 41.8%, respectively. This demonstrates a relatively overwhelming reduction in friction between the two surfaces in slipping conditions.

One can be explained by the kinematic viscosity of the lubricated agent that strongly affects the force parallel to the relative moving of the two surfaces (friction force) regarding the Reynolds equation [43]. This theme of theory seems not to limit only fluid film lubrication but also boundary lubrication, as seen from this work. The significantly low viscosity of the neat triacetin (9.32 cSt at 40 °C) was added, compared to that of the base lubricant (97.7 cSt at 40 °C), which is responsible for positive effect in some work

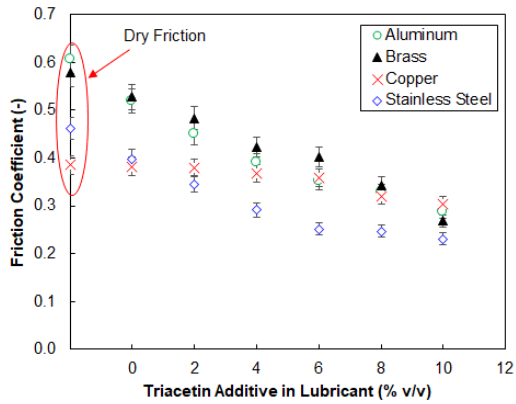

Figure 10: Friction coefficient for triacetin additive lubricated rubbing pairs of metals versus steel under boundary lubrication, error bars denote 5% error amount.

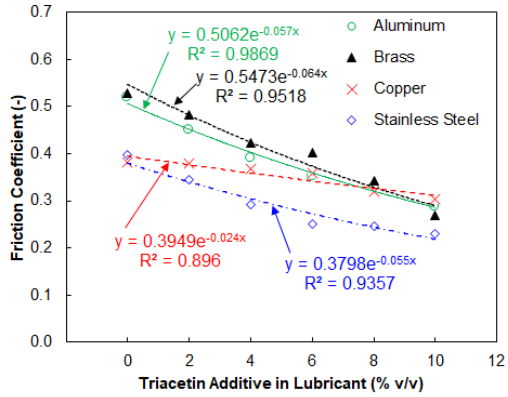

Figure 11: Friction coefficient dependency on triacetin additive amount in lubricant.

that requires lowering the friction force. However, different degrees of friction reduction is dependent on metal rubbing pairs, as also evidently shown in Figure 10.

To explain the different extent of the friction coefficient declination for all metal pairs, regression analysis was applied to the collected data previously mentioned. Figure 11 depicts some relations between friction coefficient and triacetin additive in the lubricant. The attained data can be appropriately plotted for correlation by the exponential function as [Equation (7)]:

$$C_F = \mathrm{A}\exp(\mathrm{B}\cdot\%TA) \tag{7}$$

Where C_F is slipping friction coefficient, $\%TA$ is

triacetin additive quantity in the base lubricant in % v/v, and A and B are pre-exponential factor and exponent, respectively, depending on the type of material pairs enumerated in Table 3.

Table 3: Pre-exponential factors and exponents for the friction coefficient – triacetin additive in lubrication correlation

Specimen Materials	Pre-exponential Factor, A	Exponent, B	R^2
Aluminum	0.5062	–0.057	0.9862
Brass	0.5473	–0.064	0.9518
Copper	0.3949	–0.024	0.8960
Stainless steel	0.3798	–0.055	0.9357

As it can be seen in Table 3, the negative exponent B denotes the reduction in friction coefficient values with the increasing amount of triacetin in the lubricant. Furthermore, the most negative exponent B is brass; this also demonstrates the most reduction in the friction coefficient (49.2% reduction) by up to 10% triacetin additive. When comparing with the aluminum-steel pair, the subsequent results did not ignificantly affect the copper-steel pair. This is confirmed by the exponent B for copper that is less negative (–0.024) than aluminum (–0.057). These quantitative effects of adding triacetin into the lubricant correspond to the previous result explanation in Section 3.3. Compared to the aluminum rod, the copper rod used in the test has a higher surface tension that relates to higher wettability [39]. With this higher wettability, the lubricant can be easier to insert between the two metal surfaces (copper rod and steel rollers) even with a greater proportion of triacetin additive. This yields a friction coefficient reduction rate of the copper-steel pair to be lower than that of the aluminum-steel combination.

In aspects of commercial or traditional additives in common use at present, there are three types of friction modifier additive: organic friction modifiers, organomolybdenum, and functional polymers [44]. Under particular lubrication conditions, the friction coefficient results for this study are higher than those reported in [45]. By testing on a high-frequency reciprocating rig (HFRR), the steel ball and steel disc under a certain friction environment provided the friction coefficients in the range of approx. 0.03 to 0.12 for those three types of friction modifier additive. The multifold differences result from variations in the test method, rubbing pair materials, load, additive's composition and amount based lubricant, and so on.

From the attained results that show benefits of triacetin in reducing friction, other precautions for lubrication properties such as wear metal, dispersion, and so on should be aware and proven before using. It also has to note that triacetin is an oxygenated compound that may oxidize in some circumstances; acidity, moisture, and foam formations must be concerned. These critical attributes would be accomplished for future work.

4 Conclusions

This work investigates the use of triacetin as an additive to lubricant that affects slipping friction between metal pairs of steel rollers versus aluminum, brass, copper, and stainless steel under boundary lubrication. The base lubricant was first examined for temperature and viscosity relationship that the viscosity of the oil is nonlinear, in reverse to the temperatures between 40 and 100 °C. The temperature-dependent viscosity of the oil can be expressed by the Arrhenius equation, while the kinematic viscosity of the neat triacetin additive derived from the synthesis was far lower than that of the base lubricant. From the FE-SEM imaging, coating with 10% triacetin additive in lubricant to form boundary lubrication condition reveals roughness periphery on selected metal surface textures filled by lubricant with the triacetin additive. The surface texture grooves of the softer aluminum and copper were shallower after being covered by the lubricant with the additive. The dry slipping friction coefficient over steel rollers with the rod types: copper, stainless steel, brass, and aluminum are in order from the minimum to maximum values of 0.38, 0.46, 0.57, and 0.60, respectively. The friction coefficient of copper-steel pair lower than that of aluminum-steel pair is related to high surface tension, wettability, and a fraction of grain boundary. In comparison to 0% triacetin addition, the steel roller combinations with aluminum, brass, copper, and stainless steel undergoing boundary lubrication with 10% triacetin additive in the lubricant are shown to reduce the slipping friction coefficient by 44.6, 49.2, 20.4, and 41.8%, respectively. The friction coefficients when mixing the base lubricant with the low viscosity triacetin additive, varying between 0 and 10% v/v, were founded to decline throughout

the range and can be represented by the reverse exponential function.

Acknowledgements

The authors would like to acknowledge Kasetsart University Research and Development Institute for the research funding (Grant Number: V-P(D)42.60). This research is supported in part by the Graduate Program Scholarship from The Graduate School, Kasetsart University (Grant Number: GS17102562). Kasetsart University Faculty of Science is also acknowledged for FE-SEM imaging, commissioned by Assistant Professor Dr. Krit Won-in.

References

[1] B. Gurrutxaga-Lerma, "On the transient planar contact problem in the presence of dry friction and slip," *International Journal of Solids and Structures*, vol. 193–194, pp. 314–327, Jun. 2020, doi: 10.1016/j.ijsolstr.2020.02.031.

[2] H. S. Han and K. H. Lee, "Experimental verification of the mechanism on stick-slip nonlinear friction induced vibration and its evaluation method in water-lubricated stern tube bearing," *Ocean Engineering*, vol. 182, pp. 147–161, Jun. 2019, doi: 10.1016/j.oceaneng.2019.04.078.

[3] E. Larsson, P. Olander, and S. Jacobson, "Boric acid as fuel additive – Friction experiments and reflections around its effect on fuel saving," *Tribology International*, vol. 128, pp. 302–312, Dec. 2018, doi: 10.1016/j.triboint.2018.07.004.

[4] F. L. G. Borda, S. J. R. De Oliveira, L. M. S. M. Lazaro, and A. J. K. Leiróz, "Experimental investigation of the tribological behavior of lubricants with additive containing copper nanoparticles," *Tribology International*, vol. 117, pp. 52–58, Jan. 2018, doi: 10.1016/j.triboint.2017.08.012.

[5] D. Li, D. Botto, C. Xu, T. Liu, and M. Gola, "A micro-slip friction modeling approach and its application in underplatform damper kinematics," *International Journal of Mechanical Sciences*, vol. 161–162, Oct. 2019, Art. no. 105029, doi: 10.1016/j.ijmecsci.2019.105029.

[6] R. C. Flicek, R. Ramesh, and D. A. Hills, "A complete frictional contact: The transition from normal load to sliding," *International Journal of Engineering Science*, vol. 92, pp. 18–27, Jul. 2015, doi: 10.1016/j.ijengsci.2015.03.006.

[7] N. Antoni, "A further analysis on the analogy between friction and plasticity in solid mechanics," *International Journal of Engineering Science*, vol. 121, pp. 34–51, Dec. 2017, doi: 10.1016/j.ijengsci.2017.08.012.

[8] A. Lu, C. Yin, and N. Zhang, "Analytic stress solutions for a lined circular tunnel under frictional slip contact conditions," *European Journal of Mechanics - A/Solids*, vol. 75, pp. 10–20, May–Jun. 2019, doi: 10.1016/j.euromechsol.2019.01.008.

[9] J. A. S. Malik, S. Koetniyom, A. Lamjahdy, and B. Markert, "Study of temperature and wear variations of aluminium in general dry sliding contact," *KMUTNB International Journal of Applied Science and Technology*, vol. 11, no. 1, pp. 63–72, 2018, doi: 10.14416/j.ijast.2017.12.006.

[10] X. C. Wang, B. Huang, R. L. Wang, J. L. Mo, and H. Ouyang, "Friction-induced stick-slip vibration and its experimental validation," *Mechanical Systems and Signal Processing*, vol. 142, Aug. 2020, Art. no. 106705, doi: 10.1016/j.ymssp.2020.106705.

[11] E. Pasternak, A. Dyskin, and I. Karachevtseva, "Oscillations in sliding with dry friction. Friction reduction by imposing synchronised normal load oscillations," *International Journal of Engineering Science*, vol. 154, Sep. 2020, Art. no. 103313, doi: 10.1016/j.ijengsci.2020.103313.

[12] Ö. Dincel, I. Simsek, and D. Özyürek, "Investigation of the wear behavior in simulated body fluid of 316L stainless steels produced by mechanical alloying method," *Engineering Science and Technology, an International Journal*, vol. 24, no. 1, pp. 35–40, Feb. 2021, doi: 10.1016/j.jestch.2020.12.001.

[13] Z. Xu, W. Lou, G. Zhao, M. Zhang, J. Hao, and X. Wang, "Pentaerythritol rosin ester as an environmentally friendly multifunctional additive in vegetable oil-based lubricant," *Tribology International*, vol. 135, pp. 213–218, Jul. 2019, doi: 10.1016/j.triboint.2019.02.038.

[14] N. Shaigan, W. S. Neill, J. Littlejohns, D. Song, and S. Lafrance, "Adsorption of lubricity improver additives on sliding surfaces," *Tribology*

International, vol. 141, Jan. 2020, Art. no. 105920, doi: 10.1016/j.triboint.2019.105920.

[15] P. Lan, L. L. Iaccino, X. Bao, and A. A. Polycarpou, "The effect of lubricant additives on the tribological performance of oil and gas drilling applications up to 200 °C," *Tribology International*, vol. 141, Jan. 2020, Art. no. 105896, doi: 10.1016/j.triboint.2019.105896.

[16] T. Massoud, R. P. De Matos, T. Le Mogne, M. Belin, M. Cobian, B. Thiébaut, S. Loehlé, F. Dahlem, and C. Minfray, "Effect of ZDDP on lubrication mechanisms of linear fatty amines under boundary lubrication conditions," *Tribology International*, vol. 141, Jan. 2020, Art. no. 105954, doi: 10.1016/j.triboint.2019.105954.

[17] T. I. Zohdi, "On the reduction of heat generation in lubricants using microscale additives," *International Journal of Engineering Science*, vol. 62, pp. 84–89, Jan. 2013, doi: 10.1016/j.ijengsci.2012.08.001.

[18] K. Mahmood, M. Sajid, N. Ali, and T. Javed, "Heat transfer analysis in the time-dependent slip flow over a lubricated rotating disc," *Engineering Science and Technology, an International Journal*, vol. 19, no. 4, pp. 1949–1957, Dec. 2016, doi: 10.1016/j.jestch.2016.07.009.

[19] P. Wen, Y. Lei, W. Li, and M. Fan, "Two-dimension layered nanomaterial as lubricant additives: Covalent organic frameworks beyond oxide graphene and reduced oxide graphene," *Tribology International*, vol. 143, Mar. 2020, Art. no. 106051, doi: 10.1016/j.triboint.2019.106051.

[20] Y. Cui, M. Ding, T. Sui, W. Zheng, G. Qiao, S. Yan, and X. Liu, "Role of nanoparticle materials as water-based lubricant additives for ceramics," *Tribology International*, vol. 142, Feb. 2020, Art. no. 105978, doi: 10.1016/j.triboint.2019.105978.

[21] S. Karnjanakom, P. Maneechakr, C. Samart, and G. Guan, "Ultrasound-assisted acetylation of glycerol for triacetin production over green catalyst: A liquid biofuel candidate," *Energy Conversion and Management*, vol. 173, pp. 262–270, Oct. 2018, doi: 10.1016/j.enconman.2018.07.086.

[22] L. Zhou, E. Al-Zaini, and A. A. Adesina, "Catalytic characteristics and parameters optimization of the glycerol acetylation over solid acid catalysts," *Fuel*, vol. 103, pp. 617–625, Jan. 2013, doi: 10.1016/j.fuel.2012.05.042.

[23] J. S. Ribeiro, D. Celante, L. N. Brondani, D. O. Trojahn, C. Da Silva, and F. De Castilhos, "Synthesis of methyl esters and triacetin from macaw oil (*Acrocomia aculeata*) and methyl acetate over γ-alumina," *Industrial Crops and Products*, vol. 124, pp. 84–90, Nov. 2018, doi: 10.1016/j.indcrop.2018.07.062.

[24] B. T. F. de Mello, C. P. Trentini, N. Postaue, and C. D. Silva, "Sequential process for obtaining methyl esters and triacetin from crambe oil using pressurized methyl acetate," *Industrial Crops and Products*, vol. 147, May 2020, Art. no. 112233, doi: 10.1016/j.indcrop.2020.112233.

[25] C. Odibi, M. Babaie, A. Zare, M. N. Nabi, T. A. Bodisco, R. J. Brown, "Exergy analysis of a diesel engine with waste cooking biodiesel and triacetin," *Energy Conversion and Management*, vol. 198, Oct. 2019, Art. no. 111912, doi: 10.1016/j.enconman.2019.111912.

[26] X. Dreux, J.-C. Majestéa, C. Carrot, A. Argoud, and C. Vergelati, "Viscoelastic behaviour of cellulose acetate/triacetin blends by rheology in the melt state," *Carbohydrate Polymers*, vol. 222, Oct. 2019, Art. no. 114973, doi: 10.1016/j.carbpol.2019.114973.

[27] C. Delesma, R. Castillo, P. Y. Sevilla-Camacho, P. J. Sebastian, and J. Muñiz, "Density functional study on the transesterification of triacetin assisted by cooperative weak interactions via a gold heterogeneous catalyst: Insights into biodiesel production mechanisms," *Fuel*, vol. 202, pp. 98–108, Aug. 2017, doi: 10.1016/j.fuel.2017.04.022.

[28] A. Zare, M. N. Nabi, T. A. Bodisco, F. M. Hossain, M. M. Rahman, Z. D. Ristovski, and R. J. Brown, "The effect of triacetin as a fuel additive to waste cooking biodiesel on engine performance and exhaust emissions," *Fuel*, vol. 182, pp. 640–649, Oct. 2016, doi: 10.1016/j.fuel.2016.06.039.

[29] N. Binhayeeding, S. Klomklao, and K. Sangkharak, "Utilization of waste glycerol from biodiesel process as a substrate for mono-, di-, and triacylglycerol production," *Energy Procedia*, vol. 138, pp. 895–900, Oct. 2017, doi: 10.1016/j.egypro.2017.10.130.

[30] G. Dizoğlu and E. Sert, "Fuel additive synthesis by acetylation of glycerol using activated carbon/

UiO-66 composite materials," *Fuel*, vol. 281, Dec. 2020, Art. no. 118584, doi: 10.1016/j.fuel.2020.118584.

[31] M. S. Khayoon and B. H. Hameed, "Acetylation of glycerol to biofuel additives over sulfated activated carbon catalyst," *Bioresource Technology*, vol. 102, no. 19, pp. 9229–9235, Oct. 2011, doi: 10.1016/j.biortech.2011.07.035.

[32] E. Marušić-Paloka and I. Pažanin, "Effects of boundary roughness and inertia on the fluid flow through a corrugated pipe and the formula for the Darcy–Weisbach friction coefficient," *International Journal of Engineering Science*, vol. 152, Jul. 2020, Art. no. 103293, doi: 10.1016/j.ijengsci.2020.103293.

[33] Q. Xu, W. Tao, S. Qu, and Q. Yang, "A cohesive zone model for the elevated temperature interfacial debonding and frictional sliding behavior," *Composites Science and Technology*, vol. 110, pp. 45–52, Apr. 2015, doi: 10.1016/j.compscitech.2015.01.018.

[34] R. I. Taylor, N. Morgan, R. Mainwaring, and T. Davenport, "How much mixed/boundary friction is there in an engine - and where is it?," *Proceedings of the Institution of Mechanical Engineers, Part J: Journal of Engineering Tribology*, vol. 234, no. 10, pp. 1563–1579, Sep. 2019, doi: 10.1177/1350650119875316.

[35] G. Xu, Y. Zhao, M. Li, Y. Hu, and L. Lin, "Effect of lubricant additives on the oxidation characteristics of diesel engine particulate matter," *International Journal of Chemical Engineering*, vol. 2020, Nov. 2020, Art. no. 8867515, doi: 10.1155/2020/8867515.

[36] A. Messaâdi, N. Dhouibi, H. Hamda, F. B. M. Belgacem, Y. H. Adbelkader, N. Ouerfelli, and A. H. Hamzaoui, "A new equation relating the viscosity Arrhenius temperature and the activation energy for some Newtonian classical solvents," *Journal of Chemistry*, vol. 2015, May 2015, Art. no. 163262, doi: 10.1155/2015/163262.

[37] D.-H. Cho, B. Bhushan, and J. Dyess, "Mechanisms of static and kinetic friction of polypropylene, polyethylene terephthalate, and high-density polyethylene pairs during sliding," *Tribology International*, vol. 94, pp. 165–175, Feb. 2016, doi: 10.1016/j.triboint.2015.08.027.

[38] R. -M. Wang, S. -R. Zheng, and Y. -P. Zheng, *Polymer Matrix Composites and Technology*. England: Woodhead Publishing, 2011.

[39] V. R. Sastri, *Plastics in Medical Devices: Properties, Requirements, and Applications*, 2nd ed. New York: William Andrew, 2013.

[40] N. Adachi, Y. Matsuo, Y. Todaka, M. Fujimoto, N. Hino, M. Mitsuhara, Y. Oba, Y. Shiihara, Y. Umeno, and M. Nishida, "Effect of grain boundary on the friction coefficient of pure Fe under the oil lubrication," *Tribology International*, vol. 155, Mar. 2021, Art. no. 106781, doi: 10.1016/j.triboint.2020.106781.

[41] J. J. Valencia and P. N. Quested, "Thermophysical properties," *ASM Handbook*, vol. 15, Oct. 2008, doi: 10.31399/asm.hb.v15.a0005240.

[42] B. J. Keene, "Review of data for the surface tension of pure metals," *International Materials Reviews*, vol. 38, pp. 157–192, Jul. 2013, doi: 10.1179/imr.1993.38.4.157.

[43] K. Ono, "Modified Reynolds equations for thin film lubrication analysis with high viscosity surface layers on both solid surfaces and analysis of micro-tapered bearing," *Tribology International*, vol. 151, Nov. 2020, Art. no. 106515, doi: 10.1016/j.triboint.2020.106515.

[44] H. Spikes, "Friction modifier additives," *Tribology Letters*, vol. 60, Sep. 2015, Art. no. 5, doi: 10.1007/s11249-015-0589-z.

[45] J. Guegan, M. Southby, and H. Spikes, "Friction modifier additives, synergies and antagonisms," *Tribology Letters*, vol. 67, Jun. 2019, Art. no. 83, doi: 10.1007/s11249-019-1198-z.